Chemosphere 168 (2017) 638–647

Contents lists available at ScienceDirect

Chemosphere

journal homepage: www.elsevier.com/locate/chemosphere

Electrochemical mineralization of cephalexin using a conductive diamond anode: A mechanistic and toxicity investigation

Douglas A.C. Coledam [a], Marília M.S. Pupo [b], Bianca F. Silva [c], Adilson J. Silva [d], Katlin I.B. Eguiluz [b], Giancarlo R. Salazar-Banda [b], José M. Aquino [a, *]

[a] Departamento de Química, Universidade Federal de São Carlos, C.P. 676, 13560-970 São Carlos, SP, Brazil
[b] Instituto de Tecnologia e Pesquisa/Programa de Pós-graduação em Engenharia de Processos, Universidade Tiradentes, 49032-490 Aracaju, SE, Brazil
[c] Instituto de Química de Araraquara, Departamento de Química Analítica, Universidade Estadual Paulista, 14800-900 Araraquara, SP, Brazil
[d] Departamento de Engenharia Química, Universidade Federal de São Carlos, C.P. 676, 13560-970 São Carlos, SP, Brazil

HIGHLIGHTS

- Cephalexin (CEX) antibiotic is a potential contaminant to the environment.
- Use of boron-doped diamond anode led to CEX mineralization.
- CEX molecule underwent several hydroxylation reactions before CO_2.
- Growth inhibition of *E. coli* decreased after rupture of the β-lactam ring.

ARTICLE INFO

Article history:
Received 13 September 2016
Received in revised form
2 November 2016
Accepted 3 November 2016
Available online 12 November 2016

Handling Editor: E. Brillas

Keywords:
Boron-doped diamond
Hydroxylation reactions
Diffusion controlled process
Escherichia coli
Toxicity assays

ABSTRACT

The contamination of surface and ground water by antibiotics is of significant importance due to their potential chronic toxic effects to the aquatic and human lives. Thus, in this work, the electrochemical oxidation of cephalexin (CEX) was carried out in a one compartment filter-press flow cell using a boron-doped diamond (BDD) electrode as anode. During the electrolysis, the investigated variables were: supporting electrolyte (Na_2SO_4, NaCl, $NaNO_3$, and Na_2CO_3) at constant ionic strength (0.1 M), pH (3, 7, 10, and without control), and current density (5, 10 and 20 mA cm^{-2}). The oxidation and mineralization of CEX were assessed by high performance liquid chromatography, coupled to mass spectrometry and total organic carbon. The oxidation process of CEX was dependent on the type of electrolyte and on pH of the solution due to the distinct oxidant species electrogenerated; however, the conversion of CEX and its hydroxylated intermediates to CO_2 depends only on their diffusion to the surface of the BDD. In the final stages of electrolysis, an accumulation of recalcitrant oxamic and oxalic carboxylic acids, was detected. Finally, the growth inhibition assay with *Escherichia coli* cells showed that the toxicity of CEX solution decreased along the electrochemical treatment due to the rupture of the β-lactam ring of the antibiotic.

1. Introduction

Surface and ground water contamination by synthetic organic compounds is one of the main concerns faced by the society in the 21st century (Zhang et al., 2013; Luo et al., 2014; Barbosa et al., 2016). Among the distinct classes of synthetic organic compound, such as dyes, plasticizers, personal care products, antibiotics are of significant concern due to their potential chronic toxic effects and resistance development by microorganisms (Homem and Santos, 2011; Van Doorslaer et al., 2014). The main sources of environmental contamination by antibiotics are from human excretion after previous administration, veterinary applications or by inadequate disposal of expired drugs (Homem and Santos, 2011; Kong et al., 2016). Data gathered from the National Health Surveillance Agency (ANVISA) stated that, in Brazil, the consumption of antibiotics in 2005 was up to 390 tons of amoxicillin (AMX), 184 tons of ampicillin (AMP), 163 tons of cephalexin (CEX), 133 tons of sulfamethoxazole (SMX), 45 tons of tetracycline (TET), 38 tons of norfloxacin (NOR), 30 tons of ciprofloxacin (CIP), and 27 tons of trimethoprim (TMP). At total, these compounds are responsible for

* Corresponding author.
E-mail address: jmaquino@ufscar.br (J.M. Aquino).

http://dx.doi.org/10.1016/j.chemosphere.2016.11.013
0045-6535/

>80% of the antibiotics consumed in the country (Locatelli et al., 2011).

As the conventional wastewater treatment plants are inefficient to completely remove these synthetic compounds (Zhang et al., 2013; Van Doorslaer et al., 2014; Derakhshan et al., 2016), they persist in the environment for long periods, leading to potential problems to the aquatic and human lives (Santos et al., 2010; Orias and Perrodin, 2013; Puckowski et al., 2016). Moreover, synthetic compounds, such as antibiotics, are known for their persistence in the environment, being exposed to natural degradation processes such as hydrolysis, biodegradation and photodegradation (Li and Lin, 2015). Consequently, there is the necessity to treat effluents contaminated with synthetic compounds, as well as their transformation byproducts (Escher and Fenner, 2011), before disposal into the environment in order to avoid surface water contamination (Locatelli et al., 2011; Michael et al., 2013) and production of even more toxic byproducts. There is a variety of methods to treat effluents contaminated with organic substances (Singh and Arora, 2011; Rivera-Utrilla et al., 2013; Ganzenko et al., 2014; Särkkä et al., 2015; Derakhshan et al., 2016), whose choice depends on the physical-chemistry characteristics of effluents (Oller et al., 2011). Among these methods, the electrochemical oxidation (or simply electrooxidation) might be a reasonable option (Anglada et al., 2009; Panizza and Cerisola, 2009; Brillas and Martínez-Huitle, 2015). Further, combined approaches considering methods based on the Fenton reaction (Oturan et al., 2008; Antonin et al., 2015; Cong et al., 2016; Pereira et al., 2016; Vasconcelos et al., 2016) or on photocatalysis (Sirés et al., 2014; Aquino et al., 2015; Kong et al., 2016), due to its amenable operational conditions (Radjenovic and Sedlak, 2015), are indicated treatments for effluents containing a significant range of dissolved organic compounds (Cañizares et al., 2009; Sirés et al., 2014) and with adequate conductivity.

The efficiencies of organic compound removal and electric energy consumed are strictly related to the choice of adequate electrode materials (Anglada et al., 2009; Quiroz et al., 2014; Sopaj et al., 2015) and hydrodynamic conditions used during operation. Therefore, the electrode chosen is of crucial importance in order to guarantee the system feasibility. Among the anodes proposed, boron-doped diamond (BDD) is the most investigated and well succeeded electrode material to oxidize organic molecules in distinct water matrices, such as real (Sales et al., 2013; Aquino et al., 2014a; Garcia-Segura et al., 2015a; Martín de Vidales et al., 2015) or simulated (Coledam et al., 2016) effluents, due to its ability to generate quasi-free hydroxyl radicals (HO•), high oxygen overvoltage, high resistance to corrosion in aggressive media, and resistance to deactivation (Sopaj et al., 2015). When analyzing various influence of water matrix it is important to highlight that the presence of inorganic salts, trace concentration of elements (e.g. Fe, Mg or Co), and oxidation competition with other organic and inorganic compounds are all common problematic. Therefore, the use of synthetic matrix is used as a highly controllable system in order to better understand degradation routes and the influence of systems variables (Martín de Vidales et al., 2015).

According to the literature (Guinea et al., 2009; Garcia-Segura et al., 2015b; Coledam et al., 2016), the efficiency of BDD towards degradation of organic compounds might also be related to the levels of boron doping and the ratio of sp^2 to sp^3 carbon atoms.

As has been seen in previous studies (Lizhang et al., 2016), electrochemical degradation is closely related to the concentration of organic compounds, since according to their mass transfer coefficient, most experiments report exponential drops from the anode's surface (Kapalka et al., 2009). Therefore, the conversion of organic molecules to CO_2 (mineralization) is restricted by mass transfer (Tissot et al., 2012). This problem could be overcome adjusting the applied electric current density and flow velocity during cell operation as well as using other cell geometries or turbulence promoters (Radjenovic and Sedlak, 2015). Additionally, the use of distinct electrolytes could lead to an improved oxidation (chemical oxidation) rate (Aquino et al., 2012), as oxidizing species such as active chlorine (mainly HOCl and OCl^-), persulfate, pyrophosphate and percarbonate could be produced when chloride, sulfate, phosphate and carbonate ions are used, respectively (Panizza and Cerisola, 2009; Sirés et al., 2014). However, it is unlikely that these oxidants promote complete mineralization due to their low oxidation potential.

Despite the extensive number of papers describing the application of electrochemical methods to treat contaminated effluents and synthetic solutions with a variety of organic compounds, literature on the impact of those treated effluents and solutions towards their toxicity, is still very limited (Hurwitz et al., 2014; Karci, 2014; Li and Lin, 2015). This might be due to the difficulty in finding a specific and sensitive (Guerra, 2001; Oturan et al., 2008) testing organism with respect to the target pollutant.

Thus, the aim of the present work is to investigate the electrooxidation of cephalexin (CEX), which is an antibiotic representative of the penicillin class containing a β-lactam ring, using distinct supporting electrolytes and a BDD as anode. The performance of the system will be compared through the decays of the CEX concentration (assessed by high performance liquid chromatography - HPLC) and total organic carbon (TOC), as well as the generated intermediate compounds (aromatic and short chain) by mass spectrometry analyses. The toxicity evolution of the electrolyzed solution will be followed through growth inhibition assays using the *Escherichia coli* (*E. coli*) bacterium. In addition, the experimental data of the CEX electrooxidation, using a flow cell, will be compared to a theoretical model based on a system purely controlled by mass-transport.

2. Experimental

2.1. Chemicals

All chemicals, including CEX (monohydrate 99.9% Vita Nova), Na_2SO_4 (a.r., Qhemis), NaCl (a.r., Qhemis), $NaNO_3$ (a.r., Synth), Na_2CO_3 (a.r., Synth), KH_2PO_4 (a.r., Sigma Aldrich), H_3PO_4 (85%, Mallinckrodt), $Na_2S_2O_8$ (a.r., Sigma Aldrich), carboxylic acids (a.r., Sigma Aldrich), formic acid (HPLC grade, JT Baker), tryptone (a.r., Himedia), yeast extract (a.r., Himedia), and methanol (HPLC grade, JT Baker) were used as received. Deionized water (Millipore Milli-Q system, resistivity $\geq$18.2 MΩ cm) was used for the preparation of all solutions.

2.2. BDD electrode

BDD films with 100 ppm of boron (sp^3 to sp^2 C ratio equal to 215) were synthesized through hot filament chemical vapor deposition technique on a monocrystalline Si p-doped substrate and were purchased from NeoCoat SA (Switzerland). The values in parenthesis refer to the ratio of the C atoms measured through Raman spectroscopy and were provided by the manufacturer.

2.3. Electrochemical degradation experiments

The electrochemical experiments were carried out in a one-compartment filter-press flow cell containing a BDD and an AISI 304 stainless steel plate, as anode and cathode, respectively. The exposed area of the anode was 3.54 cm × 6.71 cm. More information regarding the setup of the assembled system can be found elsewhere (Coledam et al., 2016). The investigated variables and their ranges in the electrooxidation process were: supporting electrolyte at 0.1 M of

ionic strength (i.e., 33 mM Na_2SO_4, 100 mM NaCl, 100 mM $NaNO_3$, and 33 mM Na_2CO_3), pH (3, 7, 10, and without specific control), and applied electric current density (5, 10, and 20 mA cm^{-2}). The solution pH was continuously monitored and kept constant in the desired value by additions of concentrated H_2SO_4 or NaOH solutions; the condition of "without specific control" means that no acidic or alkaline solutions were added to adjust the pH. The initial CEX concentration, as well as, flow rate (flow velocity), electrolysis time, solution temperature, and electrolyzed solution volume were fixed at 100 mg L^{-1}, 420 L h^{-1} (0.7 m s^{-1}), 360 min, 25 °C, and 1000 mL, respectively. Before any degradation electrolysis and in order to eliminate any adsorbed organic compound, the BDD anode was electrochemically pre-treated in a 0.5 M H_2SO_4 solution by applying 20 mA cm^{-2} for 15 min.

2.4. Analyses

Concentration of CEX was monitored by high performance liquid chromatography (HPLC) using a core shell C-18 reversed phase as the stationary phase (150 mm × 4.6 mm, 5 μm particle size from Phenomenex®) and a mixture of 10 mM KH_2PO_4 at pH 3 (eluent A) and methanol (eluent B) in a gradient elution mode as the mobile phase and flow rate of 1 mL min^{-1}. The gradient elution protocol started with 10% of eluent B, increasing to up to 90% after 12 min. Then, the composition of the mobile phase returned to 10% of eluent B after being kept at 90% for 2 min. The sample injection volume was 25 μL.

The intermediate compounds analyses were carried out with samples collected every 1 h until 8 h of electrolysis. The extracted samples of 2 mL were first frozen and then dried in a lyophilization system (CHRIST alpha 2–4 LD Plus) for 24 h. After this period, the samples were resuspended in 1 mL of methanol and filtered using a 0.22 μm cartridge. The intermediates formed during the CEX degradation were determined in a HPLC 1200 Agilent Technologies coupled to a mass spectrometer 3200 QTRAP (LC-MS/MS, Linear Ion Trap Quadrupole), AB SCIEX Instruments operating in a positive mode and TurboIonSpray ionization. *Lightsight*® 2.3 (Nominal Mass Metabolite ID Software, AB SCIEX) software was used to investigate all possibilities of metabolites. The software application was performed through the all ionization and fragmentation parameters optimized for the initial compound. The parameters were obtained using a direct infusion of 10 μL min^{-1} of a solution containing CEX compound (1 mg L^{-1}) in H_2O:MeOH (1:1, *V*/*V*, with 0.1% of formic acid). The parameters conditions were: curtain gas at 20 psi, ion spray at 5200 V, gas 1 and gas 2 at 50 psi, temperature of 600 °C, declustering potential of 41 V, entrance potential of 8 V and with interface heater ON. Optimized selected reaction monitoring (SRM) and fullscan experiments were automatically performed by *LightSight*® to investigate different kinds of possible reactions, such as oxidation, hydroxylation, reduction, C–C bond cleavage and others. During the LC-MS/MS analyses, the phosphate buffer used in the mobile phase was changed to water containing 0.1% of formic acid. The injection volume was 20 μL and the samples collected at 0, 1, 2 and 3 h were diluted to one third before injection.

Short chain carboxylic acids were also determined by HPLC for the optimized electrolysis condition. A Rezek ROA-H™ column from Phenomenex® was used as the stationary phase and a 2.5 mM H_2SO_4 solution as the mobile phase at 0.5 mL min^{-1}. The carboxylic acids were identified through comparison of retention times with previously analyzed standards and by UV detection at 210 nm. The injection volume and column temperature were maintained at 25 μL and 23 °C, respectively.

The toxicity test with *E. coli* was carried out with electrolyzed samples extracted each 1.5 h and at the beginning of the electrochemical experiment. Tryptone, yeast extract, and NaCl (Lennox LB broth) were added to each sample to a final concentration of 10, 5, and 5 g L^{-1}, respectively, and these solutions were filter-sterilized. An overnight culture of *E. coli* K12 MG1655 was used to inoculate 15 mL tubes containing 3 mL of samples, with 9×10^5 cfu mL^{-1} (cfu, colony forming units). Three tubes containing only LB medium were also inoculated to be used as negative controls. All tubes (in triplicate for each analyzed electrolysis time) were incubated at 37 °C for 24 h at 200 rpm. After this period, *E. coli* growth was analyzed by measuring the absorbance of solutions at 600 nm, and the toxicity of samples was assessed through the inhibition index (*I*), calculated according to Silambarasan and Vangnai (2016):

$$I = \left(\frac{A_0 - A}{A_0}\right) \times 100 \quad (1)$$

where A_0 and A are the absorbance values in the absence (control samples) and presence (samples from all the investigated electrolysis time) of CEX, respectively. The minimum inhibitory concentration (MIC) of CEX was determined by the micro-dilution method. Successive dilutions (dilution factor of 2) of a filter-sterilized LB medium containing 100 mg L^{-1} CEX were applied to a 96-well microplate and test wells were inoculated with 2×10^5 cfu mL^{-1} of an overnight culture of *E. coli* K12 MG1655. After incubation at 37 °C for 24 h, bacterial growth was analyzed by adding 50 μL of a 0.2 mg mL^{-1} p-iodonitrotetrazolium chloride solution to each well and further incubation at 37 °C for 30 min. Bacterial growth was visualized by a color change (from colorless to reddish pink), whereas clear wells indicated growth inhibition. The assay was repeated twice with three replicates each. The minimum CEX concentration where the growth of *E. coli* was confirmed to be inhibited (no color change) was 12.5 mg L^{-1}. This MIC value is in agreement with the one reported by Giacomino et al. (2012), whose value was equal to 16 mg L^{-1}.

The extent of mineralization (i.e. conversion to CO_2 and H_2O) was monitored by total organic carbon (TOC) measurements every 1 h after sampling and dilution of 5 mL of the electrolyzed solution using a GE Sievers Innovox analyzer. The TOC determination was carried out after mixing the electrolyzed sample with H_3PO_4 (6 M) and $Na_2S_2O_8$ (30% *m*/*m*) solutions. The oxidation was accomplished after the temperature and pressure corresponding to the supercritical point of water was reached. The TOC content was given by subtraction of the measured values of inorganic and total carbon, in terms of generated CO_2 and after comparison with a previously determined calibration curve, using a nondispersive infrared detector.

The mineralization current efficiency (*MCE*) was calculated according to the work of Brillas et al. (2009):

$$MCE = \frac{\Delta(TOC)_t nFV}{4.32 \times 10^7 mIt} \times 100 \quad (2)$$

where $\Delta(TOC)_t$ is the measured TOC removal (mg carbon L^{-1}) after a certain time, *t* (h), *n* is the number of exchanged electrons considering that the total electric applied charge was consumed in the mineralization process (see eq. (3)), *F* the Faraday constant (96,485 C mol^{-1}), 4.32×10^7 is a conversion factor (3600 s h^{-1} × 12,000 mg mol^{-1} carbon), *V* the electrolyzed solution volume (L), *m* the number of carbon atoms of the CEX molecule, and *I* the applied electric current (A).

$$C_{16}H_{17}N_3O_4S + 41H_2O \rightarrow 16CO_2 + 99H^+ + 3NO_3^- + SO_4^{-2} + 94e^- \quad (3)$$

The extent of total electrochemical combustion (φ) (Miwa et al., 2006) was calculated through the ratio between the percentages of

CEX and TOC samples taken at each 1 h of electrolysis in the optimized conditions:

$$\varphi = \frac{\%[TOC]_{removed}}{\%[CEX]_{removed}} \quad (4)$$

The φ value gives an indication of the extent to which the CEX molecules are being converted to CO_2 or to other intermediate compounds. So, this parameter can assume values between 0 and 1, which means no combustion or total combustion with respect to the initial compound, respectively.

The energy consumption per unit mass of TOC (w) for the electrochemical mineralization process was calculated according to Brillas et al. (2009):

$$w = \left(\frac{UIt}{\Delta[TOC]V}\right) \quad (5)$$

where U is the cell voltage (V), I the applied electric current (A), t the reaction time (h), Δ[TOC] the concentration variation of TOC (mg L^{-1}) after a certain reaction time, and V the electrolyzed solution volume (L).

3. Results and discussion

3.1. Effect of operational variables

Fig. 1 shows the relative concentration decay of CEX (100 $[CEX]_{rel}$; $[CEX]_{rel} = [CEX]_t/[CEX]_0$ where $[CEX]_t$ and $[CEX]_0$ are the CEX concentration at time t and at the beginning of the electrolysis) and TOC (100$[TOC]_{rel}$; $[TOC]_{rel} = [TOC]_t/[TOC]_0$ where $[TOC]_t$ and $[TOC]_0$ are the TOC concentration at time t and at the beginning of the electrolysis) as a function of electrolysis time for distinct salts used as supporting electrolyte at constant ionic strength (0.1 M). A theoretical line based on a process purely controlled by mass transfer, whose main parameter is the mass transfer coefficient (k_m), was also included to show the important contribution of indirect processes (chemical oxidation) on the CEX oxidation and mineralization performances. The k_m value (3.09×10^{-5} m s^{-1}) was calculated after determination of the thickness of the stagnant layer (2.32×10^{-5} m), by a simple electrochemical assay based on the

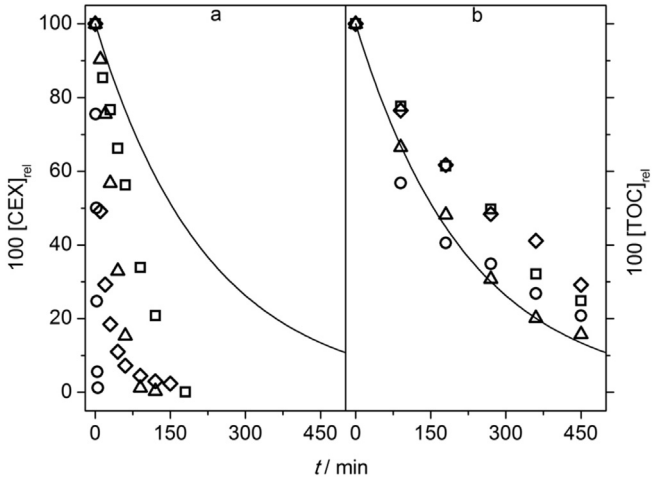

Fig. 1. – Relative concentration decay of a) CEX (100 $[CEX]_{rel}$) and b) TOC (100$[TOC]_{rel}$) as a function of electrolysis time using distinct salts as supporting electrolyte at a constant ionic strength (0.1 M): (□) Na_2SO_4, (○) NaCl, (△) $NaNO_3$, (◇) Na_2CO_3. (———) theoretical line based on a purely mass transport controlled process. Conditions of the electrolysis: 25 °C and using 20 mA cm^{-2}.

$Fe(CN)_6^{4-}/Fe(CN)_6^{3-}$ redox pair (Cañizares et al., 2006), and of the diffusion coefficient of the CEX (7.17×10^{-10} m^2 s^{-1}) using a diaphragm cell. Thus, the theoretical first order kinetic constant and exponential decay can be calculated according to previous reports (Coledam et al., 2014, 2016).

It is interesting to note that the oxidation process, which is related to small modifications on the initial CEX molecule, is a faster kinetic process than the one based on mass transfer probably due to the contribution of oxidant species produced during the electrolysis. Thus, all salts used led to higher removal rates than the theoretical line, i.e. the oxidation is not limited to the surface of the anode. Similar results are commonly seen for electrochemical degradation on BDD, as was reported recently by Lizhang et al. (2016), while studying the kinetics of phenol electrochemical oxidation highlighting the importance of bulk reactions during total mineralization.

Moreover, the use of Cl^- ions led to the highest rate of oxidation (only a few minutes to complete oxidation) within the tested salts, as a consequence of the generation of active chlorine (mainly HOCl and OCl^-), which may react through addition, oxidation or substitution reactions (Deborde and von Gunten, 2008) in a non-selective way. When carbonate, sulfate, and nitrate based electrolytes were used, the pseudo-first order kinetic constants gradually increased in that order, but their values remained lower than the one using Cl^- ions (see the pseudo-first order kinetic constants of Table SM-1, in the electronic supplementary material section).

On the other hand, the TOC decay was similar for all tested electrolytes. The TOC removal is related to a much more severe oxidation route, i.e. the molecule has to undergo many oxidation steps before a significant CO_2 conversion (Aquino et al., 2014b). Similar results were reported in previous studies (Hurwitz et al., 2014), considering that BDD is a non-active electrode and that their mineralization reaction routes are strongly associated to the generation of HO•, a close TOC decay for various electrolytes used was expected.

Moreover, as the electrogenerated oxidants (chemical oxidation) are incapable to mineralize CEX molecules, these molecules need to diffuse towards the anode surface to be oxidized and mineralized by HO•. This explains why the experimental points and theoretical line are close for the TOC removal in comparison to the data regarding the oxidation removal. The conversion of CEX and its intermediates to CO_2 is dependent on the HO• produced on the anode surface and, as expected, the extent of total electrochemical combustion (φ), which remained around 0.77, was similar for all the investigated electrolytes after 7 h (see Fig. SM-1, in the electronic supplementary material section). The remaining experiments were carried out using a sulfate medium (33 mM Na_2SO_4) to avoid the possible electrogeneration of toxic organic (Garcia-Segura et al., 2015a) and inorganic (Bergmann et al., 2009; Lin et al., 2016) compounds, and also to avoid fouling of the BDD anode by nitrate substituted intermediates (Murugananthan et al., 2011).

Fig. 2 shows the 100$[CEX]_{rel}$ and 100$[TOC]_{rel}$ as a function of electrolysis time for distinct values of investigated pH in sulfate medium. Once again, different profiles can be observed for the oxidation and mineralization processes. During the CEX oxidation, all the experimental data exhibited higher rates than the theoretical one due to the contribution of the electrogenerated oxidants (chemical oxidation process) such as H_2O_2 and $S_2O_8^{2-}$, as discussed above and also showed experimentally in other works (Coledam et al., 2016). In addition, the oxidation process was dependent on the pH value: neutral to acidic solutions and the ones with no control (variation range: from 6.5 to 3.0) led to the highest oxidation rates (see Table SM-2, in the electronic supplementary material section), which slightly diminished when alkaline solutions were used. This behavior might be due to the distinct pK_a values of the

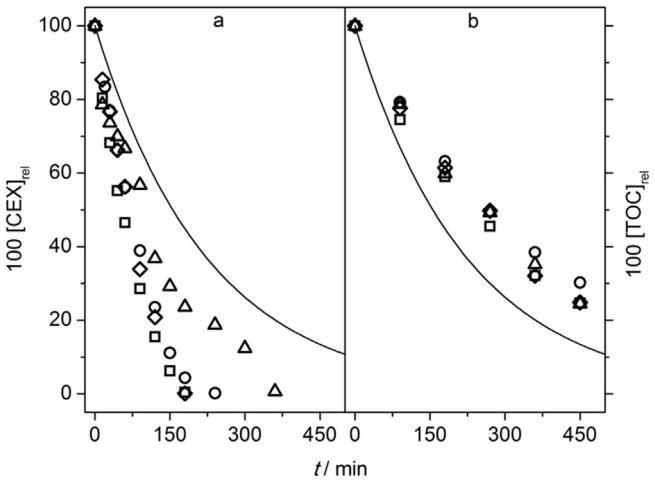

Fig. 2. – Relative concentration decay of a) CEX (100 $[CEX]_{rel}$) and b) TOC (100$[TOC]_{rel}$) as a function of electrolysis time at distinct pH values: (□) 3, (○) 7, (△) 10, and (◇) no control. Conditions of the electrolysis: 25 °C and using 20 mA cm^{-2} in the presence of Na_2SO_4 0.033 M.

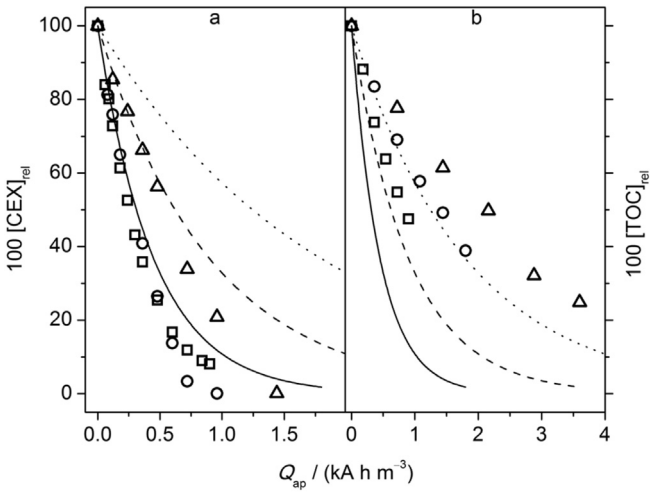

Fig. 3. – Relative concentration decay of a) CEX (100 $[CEX]_{rel}$) and b) TOC (100$[TOC]_{rel}$) as a function of electric applied charge per unit volume of electrolyzed solution (Q_{ap}) using distinct current density values: (□) 5, (○) 10, and (△) 20 mA cm^{-2}. Theoretical lines based on a purely mass transport controlled process using (———) 10, (– – –) 20, and (• • •) 30 mA cm^{-2}. Conditions of the electrolysis: no pH control at 25 °C and in the presence of Na_2SO_4 0.033 M.

CEX molecule (5.2 and 7.3 (Giacomino et al., 2012)), which is in the ionic form at pH 10 and could have influenced the interaction with electrogenerated oxidants or even their oxidation power. For the mineralization process, the experimental data exhibited a lower rate than the theoretical one and no pH dependence is observed. Clearly, that process seems to not depend on the ionic character of the CEX molecule (similar diffusion coefficients), since the conversion to CO_2 occurs by diffusion of CEX towards the anode surface followed by consecutive oxidation reactions mediated by HO• (reaction cage).

As discussed above, the conversion to CO_2 is limited by the diffusion of the CEX molecule and its intermediates to the anode surface to react with HO•, which might occur through several steps due to the complexity of the organic compound. As discussed in the work of Farhat et al. (2015), the mineralization of CEX could also be mediated by sulfate radicals ($SO_4^{\bullet -}$) in acidic solutions, which are produced from oxidation of sulfate ions or by their reaction with HO•.

Fig. 3 shows the 100$[CEX]_{rel}$ and 100$[TOC]_{rel}$ as a function of the applied electric charge per unit volume of electrolyzed solution (Q_{ap}) for distinct values of applied electric current density values investigated and without pH control. Once again, the oxidation process required a lower Q_{ap} than the mineralization process, as the conversion to CO_2 only occurs on the surface of the BDD anode. It is interesting to observe that the rate of CEX oxidation significantly increased from 5 to 10 mA cm^{-2}, and the theoretical line (considering the oxidation process at 5 mA cm^{-2}) was very close to the experimental points at 5 mA cm^{-2}. That behavior might be due to the limiting current density (j_{lim}) value, which is equal to 8 mA cm^{-2}. Thus, when current densities higher than j_{lim} are used, the excess electric energy is consumed by the side reaction of O_2 evolution, as well as, production of oxidants. This last point explains why there is a significant disagreement between the theoretical and experimental points at 20 mA cm^{-2}. Previous reports (Carlesi Jara and Fino, 2010) highlight that the current density is mainly influenced by the initial contaminant concentration and mass transport limitation inside the electrochemical reactor, which is in accordance with our findings.

In the case of TOC removal, all the experimental values remained above the theoretical line due to the several oxidation steps that the CEX molecule, and its intermediates, need to overcome before conversion to CO_2. Moreover, the oxidation promoted by the electrogenerated oxidants is incapable to generate significant mineralization, which could explain the higher Q_{ap} required for the mineralization process. Table SM-3, in the electronic supplementary material section, shows the obtained pseudo-first order kinetic constants for the oxidation and mineralization processes. As expected, the *k* values increase with the applied current density values. The obtained *MCE* and *w* values as a function of TOC removal can be seen in Fig. SM-2 in the electronic supplementary material section. As the system is under mass transfer control, the use of high electric current densities led to low values of *MCE* and a consequent increase of the side reaction of O_2 evolution. Moreover, increasingly high *w* values were attained at high current densities.

3.2. Intermediate compounds and toxicity assays

Table 1 shows some of the main detected intermediate compounds by LC-MS/MS analyses that were generated during electrooxidation of CEX using a BDD anode (for the proposed fragmentation route of the main detected intermediates and the IUPAC names of the proposed chemical structures, see Figs. from SM-3 to SM-15 and Table SM-4, respectively, in the electronic supplementary material section). Other *m*/*z* relations were detected, but their concentration were very low to perform MS/MS analysis. An initial possible degradation pathway is also proposed in Fig. 4. It is interesting to observe that all detected intermediates result from hydroxylation (see compounds **3**, **10**, **11**, and **13**) and oxidation (see compounds **1**, **4**, and **5**) reactions in the cephem group (formed by the β-Lactam containing thiazine ring) or in the substituent methyl group (see compounds **1**, **6**, **7**, **8**, **9**, **10** **11**, **12**, and **13**). These reactions are common when advanced oxidation processes are used to oxidize and mineralize organic compounds (Klauson et al., 2010; Coledam et al., 2016).

On the other hand, the breakage of the cephem group, which is the active part of the CEX molecule and it is responsible for its antibacterial properties, occurred during the electrooxidation process, as shown by compound number **2**, which was detected after 4 h of electrolysis. The benzene and amino groups were also hydroxylated (see compounds **7**, **9**, **10**, **11** and **13**) during the

Table 1
LC-MS/MS data for the intermediate compounds detected during electrochemical oxidation of CEX using a BDD anode.

*	Molar mass/g mol^{-1}	Retention time/min	Molecular ion $[M+H]^+$/Da	Main fragment ions/Da	Proposed chemical structures
1	317	7.19	318	301, 269, 216, and 106	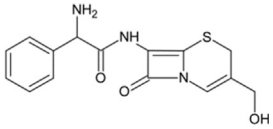
2	264	9.12	265	216, 158, 145, and 106	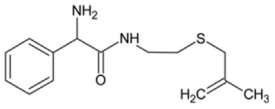
3	363 (a)	1.88	364	346, 156, and 106	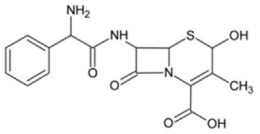
4	333	6.54	334	317, 285, 167, 144, and 132	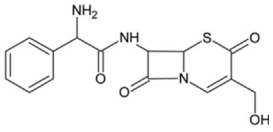
5	361	8.77	362	257, 212, 177, and 133	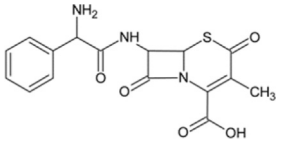
6	377 (a)	5.51	378	361, 329, 233, 218, 186, 158, and 106	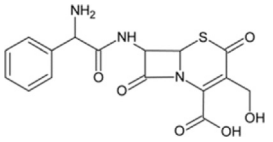
7	393	5.82	394	346, 329, and 106	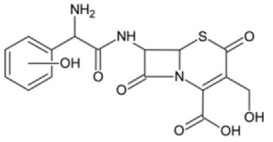
8	363 (b)	3.09	364	346, 329, 206, 156, and 106	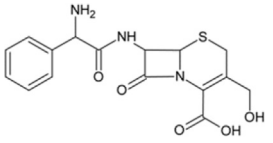
9	379	7.59	380	363, 362, 331, and 106	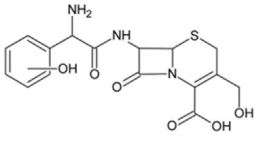
10	411	10.75	412	377, 346, 152, and 106	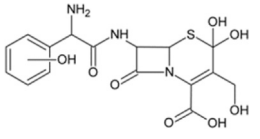
11	395	8.90	396	346, 329, 297, and 106	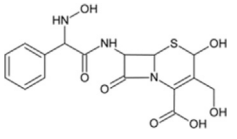

(*continued on next page*)

Table 1 (*continued*)

*	Molar mass/g mol^{-1}	Retention time/min	Molecular ion $[M+H]^+$/Da	Main fragment ions/Da	Proposed chemical structures
12	345	6.70	346	329, 285, 211, 156, and 106	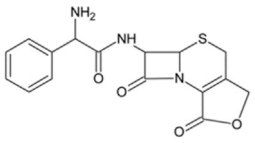
13	377 (b)	7.39	378	329, 300, 274, 156, and 106	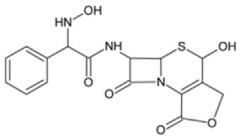

*The numbers refer to the proposed degradation pathway of Fig. 4.

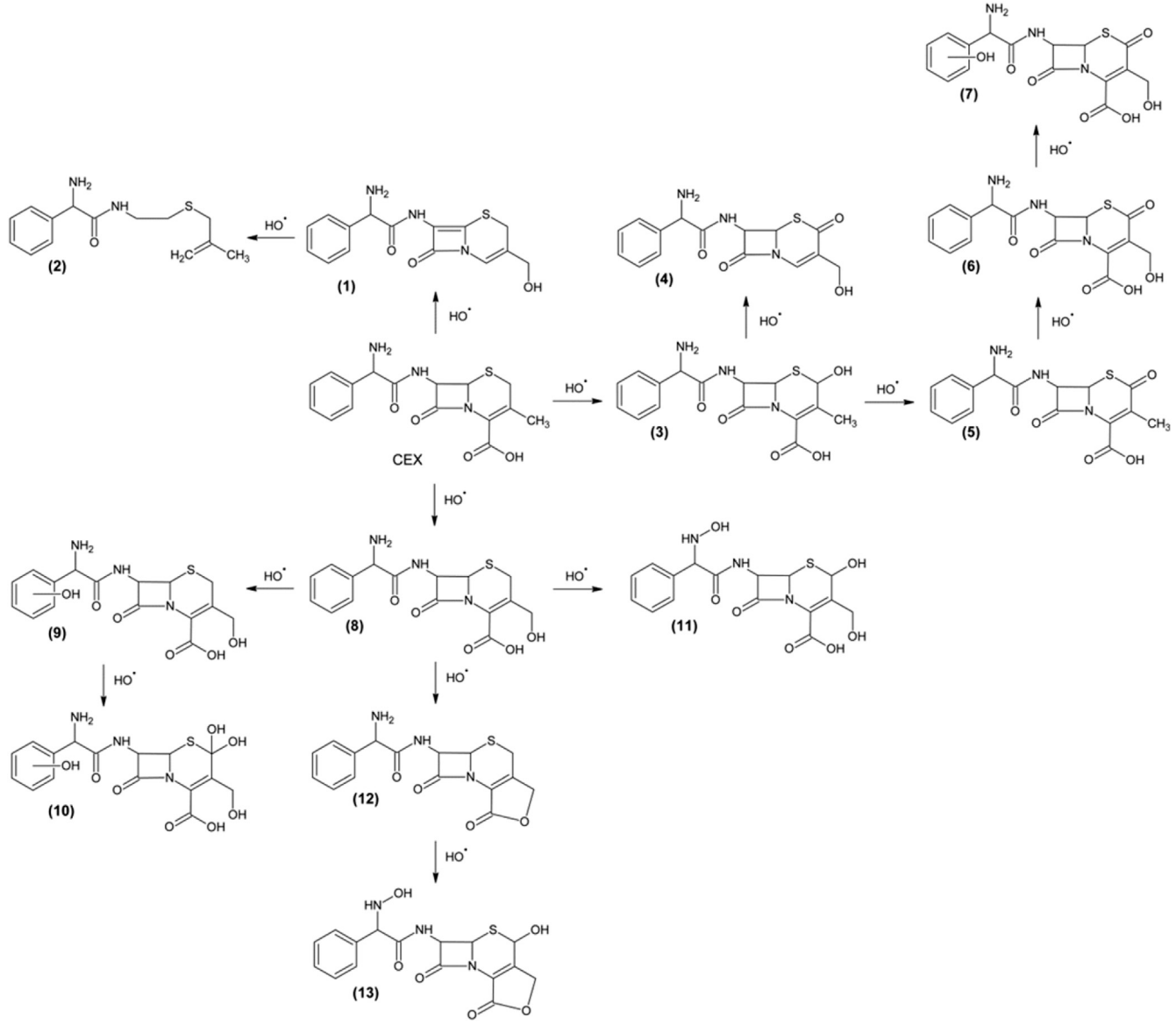

Fig. 4. – Proposed degradation pathway of CEX under electrochemical oxidation using a BDD anode. Conditions of the electrolysis: 25 °C, no pH control, and using 10 mA cm^{-2} in the presence of Na_2SO_4 0.033 M.

electrochemical process; however, no intermediate resulting from the benzene ring opening was detected. This behavior might be due to the low applied electric current density, which is close to the limiting one. Consequently, it is expected that a high conversion of

CEX molecules to its intermediates before significant conversion to carboxylic acids and CO_2, would be seen. The majority of the identified intermediates reported in this work is mainly due to hydroxylation reactions in the six-member β-lactam ring. That behavior seems to be different from the one reported by Song et al. (2008), where hydroxylation in the aromatic ring of other β-lactam antibiotics (four-member β-lactam ring compounds: Penicillin G, Penicillin V, and Amoxicilin) was predominantly when using radiolysis as an advanced oxidation process. As also reported by Rickman and Mezyk (2010), during investigation of the oxidation of four- and six-member β-lactam ring antibiotics through sulfate or hydroxyl radicals using advanced oxidation and reduction processes, the presence of sulfate radicals can promote oxidation reactions in the six-member β-lactam ring rather than on the aromatic substituent. That behavior was also observed by Dodd et al. (2010) during treatment of CEX by an ozonation process (no oxidation reaction in the aromatic substituent). Thus, this might explain the observed high number of byproducts in this work with the six-member β-lactam ring oxidized when using the electrochemical technology in the presence sulfate ions. The concentration evolution of short chain compounds (carboxylic acids in this study) resulting from consecutive oxidation steps of the CEX compound, as a function of the electrolysis time, can be seen in Fig. 5. Oxamic, oxalic, malic and propionic acids presented the highest concentration during the electrochemical treatment of CEX, even after 7 h electrolysis, and only small amounts of pyruvic, succinic and fumaric acids were detected. Clearly, there is a tendency of accumulation of recalcitrant oxamic and oxalic carboxylic acids (Garcia-Segura and Brillas, 2011) during the final stages of electrochemical oxidation of CEX. Further, it is well known and typically seen in electrolysis reaction, that oxalic acid is the last carboxylic acid that is directly transformed into CO_2 (Han et al., 2014).

Finally, Fig. 6 shows the evolution of the inhibition index (I) of *E. coli* and the CEX concentration as a function of the electrolysis time. During the initial 3 h of electrolysis, the growth of *E. coli* was completely inhibited even after diminishment of the CEX concentration below the MIC (see dashed line in Fig. 6), which occurred at 3 h of electrolysis. This might indicate that the byproducts of the CEX molecule, particularly those after successive hydroxylation reactions shown in the degradation pathway of Fig. 4, continues to inhibit the growth of *E. coli*, as the cephem group was not broken. Then, after 4 h of electrolysis, no significant growth inhibition towards the growth of *E. coli* was observed, probably due to the rupture of the β-Lactam ring of the CEX intermediates (without complete TOC abatement), as shown by compound **2** in Fig. 4. On the other hand, Dimitrakopoulou et al. (2012) showed that the antibacterial activity of amoxicillin (another antibiotic representative of the penicillin group) towards *E. coli* was only dependent on the removal of the parent compound and not on its degradation byproducts, during a photocatalytic treatment using TiO_2 and UV-A radiation. That behavior might be due to the rapid rupture of the β-lactam ring of the amoxicillin compound whose intermediates were not detected. In addition, the accumulation of oxamic and oxalic acids detected during treatment of CEX did not seem to inhibit the growth of *E. coli* cells.

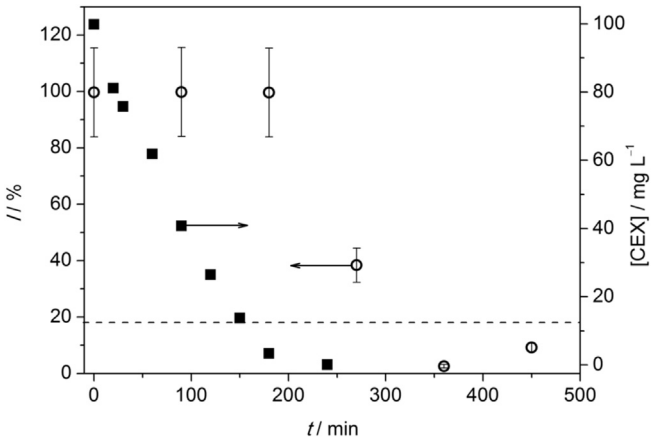

Fig. 6. – Inhibition index (I) and absolute concentration evolution of CEX ([CEX]) as a function of the electrolysis time: (○) I, (■) [CEX], and (– – –) the obtained experimental value of the minimum inhibitory concentration (MIC - see text). Conditions of the electrolysis: 25 °C, no pH control, and using 10 mA cm^{-2} in the presence of Na_2SO_4 0.033 M.

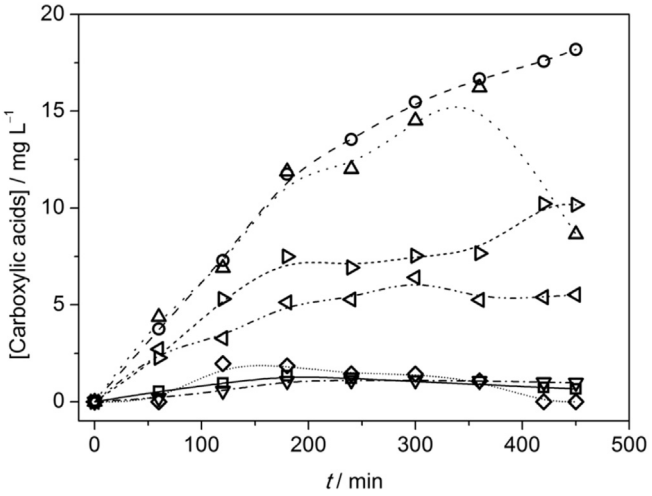

Fig. 5. – Concentration evolution of the main detected carboxylic acids as a function of electrolysis time: (▽) fumaric, (△) malic, (○) oxamic, (▷) oxalic, (◁) propionic, (□) pyruvic, and (◇) succinic acids. Conditions of the electrolysis: 25 °C, no pH control, and using 10 mA cm^{-2} in the presence of Na_2SO_4 0.033 M.

4. Conclusions

The CEX molecule and its hydroxylated intermediate compounds were completely eliminated during electrolysis using a BDD as anode. The oxidation rate of CEX using distinct salts as supporting electrolyte exhibited distinct rates due to the different types and amounts of electrogenerated oxidants; however, none of them were capable to mineralize CEX and its intermediates, which only occurred on the surface of BDD through a diffusion process. Neutral to acidic solutions led to the best removal rates of CEX; however, no significant difference was observed towards the conversion to CO_2 as the system is under mass transfer limitations. Consequently, the use of high values of electric current density is not indicated since a high energy consumption and low mineralization current efficiencies are attained. The main detected CEX intermediates were due to hydroxylation reactions in the cephem group, which remained as toxic as the parent compound. The inhibition growth of *E. coli* was limited when the cephem group, particularly the β-lactam ring, was broken. The presence and accumulation of recalcitrant oxamic and oxalic carboxylic acids did not lead to any significant inhibition towards growth of *E. coli*.

Acknowledgments

CAPES, FAPITEC, CNPq (grant numbers 310282/2013-6 and 304419/2015-0), and São Paulo Research Foundation (FAPESP, grant

number 2008/10449-7) are gratefully acknowledged for financial support and scholarships. Vita Nova is also gratefully acknowledged for supplying samples of the CEX compound.

Appendix A. Supplementary data

Supplementary data related to this article can be found at http://dx.doi.org/10.1016/j.chemosphere.2016.11.013.

References

Anglada, A., Urtiaga, A., Ortiz, I., 2009. Contributions of electrochemical oxidation to waste-water treatment: fundamentals and review of applications. J. Chem. Technol. Biotechnol. 84, 1747–1755.

Antonin, V.S., Santos, M.C., Garcia-Segura, S., Brillas, E., 2015. Electrochemical incineration of the antibiotic ciprofloxacin in sulfate medium and synthetic urine matrix. Water Res. 83, 31–41.

Aquino, J.M., Parra, K.N., Miwa, D.W., Motheo, A.J., 2015. Removal of phthalic acid from aqueous solution using a photo-assisted electrochemical method. J. Environ. Chem. Eng. 3, 429–435.

Aquino, J.M., Rocha-Filho, R.C., Ruotolo, L.A.M., Bocchi, N., Biaggio, S.R., 2014a. Electrochemical degradation of a real textile wastewater using b-PbO_2 and DSA® anodes. Chem. Eng. J. 251, 138–145.

Aquino, J.M., Rocha-Filho, R.C., Sáez, C., Cañizares, P., Rodrigo, M.A., 2014b. High efficiencies in the electrochemical oxidation of an anthraquinonic dye with conductive-diamond anodes. Environ. Sci. Pollut. Res. 21, 8442–8450.

Aquino, J.M., Rodrigo, M.A., Rocha-Filho, R.C., Sáez, C., Cañizares, P., 2012. Influence of the supporting electrolyte on the electrolyses of dyes with conductive-diamond anodes. Chem. Eng. J. 184, 221–227.

Barbosa, M.O., Moreira, N.F.F., Ribeiro, A.R., Pereira, M.F.R., Silva, A.M.T., 2016. Occurrence and removal of organic micropollutants: an overview of the watch list of EU Decision 2015/495. Water Res. 94, 257–279.

Bergmann, M.E.H., Rollin, J., Iourtchouk, T., 2009. The occurrence of perchlorate during drinking water electrolysis using BDD anodes. Electrochim. Acta 54, 2102–2107.

Brillas, E., Martínez-Huitle, C.A., 2015. Decontamination of wastewaters containing synthetic organic dyes by electrochemical methods. An updated review. Appl. Catal. B Environ. 166–167, 603–643.

Brillas, E., Sirés, I., Oturan, M.A., 2009. Electro-Fenton process and related electrochemical technologies based on Fenton's reaction chemistry. Chem. Rev. 109, 6570–6631.

Cañizares, P., García-Gómez, J., de Marcos, I.F., Rodrigo, M.A., Lobato, J., 2006. Measurement of mass-transfer coefficients by an electrochemical technique. J. Chem. Educ. 83, 1204–1207.

Cañizares, P., Paz, R., Sáez, C., Rodrigo, M.A., 2009. Costs of the electrochemical oxidation of wastewaters: a comparison with ozonation and Fenton oxidation processes. J. Environ. Manage 90, 410–420.

Carlesi Jara, C., Fino, D., 2010. Cost optimization of the current density for electro-oxidation wastewater processes. Chem. Eng. J. 160, 497–502.

Coledam, D.A.C., Aquino, J.M., Rocha-Filho, R.C., Bocchi, N., Biaggio, S.R., 2014. Influence of chloride-mediated oxidation on the electrochemical degradation of the Direct Black 22 dye using boron-doped diamond and β-PbO_2 anodes. Quim. Nova 37, 1312–1317.

Coledam, D.A.C., Aquino, J.M., Silva, B.F., Silva, A.J., Rocha-Filho, R.C., 2016. Electrochemical mineralization of norfloxacin using distinct boron-doped diamond anodes in a filter-press reactor, with investigations of toxicity and oxidation by-products. Electrochim. Acta 213, 856–864.

Cong, V.H., Sakakibara, Y., Komori, M., Kishimoto, N., Watanabe, T., Mishima, I., Ihara, I., Tanaka, T., Yoshida, Y., Ozaki, H., 2016. Recent developments in electrochemical technology for water and wastewater treatments. J. Water Environ. Technol. 14, 25–36.

Deborde, M., von Gunten, U., 2008. Reactions of chlorine with inorganic and organic compounds during water treatment-Kinetics and mechanisms: a critical review. Water Res. 42, 13–51.

Derakhshan, Z., Mokhtari, M., Babaie, F., Ahmadi, R.M., 2016. Removal methods of antibiotic compounds from aqueous environments – a review. J. Environ. Health Sustain. Dev. 1, 51–74.

Dimitrakopoulou, D., Rethemiotaki, I., Frontistis, Z., Xekoukoulotakis, N.P., Venieri, D., Mantzavinos, D., 2012. Degradation, mineralization and antibiotic inactivation of amoxicillin by UV-A/TiO_2 photocatalysis. J. Environ. Manage 98, 168–174.

Dodd, M.C., Rentsch, D., Singer, H.P., Kohler, H.-P.E., von Gunten, U., 2010. Transformation of beta-lactam antibacterial agents during aqueous ozonation: reaction pathways and quantitative bioassay of biologically-active oxidation products. Environ. Sci. Technol. 44, 5940–5948.

Escher, B.I., Fenner, K., 2011. Recent advances in environmental risk assessment of transformation products. Environ. Sci. Technol. 45, 3835–3847.

Farhat, A., Keller, J., Tait, S., Radjenovic, J., 2015. Removal of persistent organic contaminants by electrochemically activated sulfate. Environ. Sci. Technol. 49, 14326–14333.

Ganzenko, O., Huguenot, D., van Hullebusch, E.D., Esposito, G., Oturan, M.A., 2014. Electrochemical advanced oxidation and biological processes for wastewater treatment : a review of the combined approaches. Environ. Sci. Pollut. Res. 21, 8493–8524.

Garcia-Segura, S., Brillas, E., 2011. Mineralization of the recalcitrant oxalic and oxamic acids by electrochemical advanced oxidation processes using a boron-doped diamond anode. Water Res. 45, 2975–2984.

Garcia-Segura, S., Keller, J., Brillas, E., Radjenovic, J., 2015a. Removal of organic contaminants from secondary effluent by anodic oxidation with a boron-doped diamond anode as tertiary treatment. J. Hazard. Mater 283, 551–557.

Garcia-Segura, S., Vieira dos Santos, E., Martínez-Huitle, C.A., 2015b. Role of sp^3/sp^2 ratio on the electrocatalytic properties of boron-doped diamond electrodes: a mini review. Electrochem. Commun. 59, 52–55.

Giacomino, N., Cerra, M., Gumiy, D., Stiefel, S., Notaro, U., Baroni, E., Formentini, E., 2012. Pharmacokinetic-pharmacodynamic modeling of antibacterial activity of cephalexin on *E. coli* in presence of canine serum. Revue Méd. Vét. 163, 431–440.

Guerra, R., 2001. Ecotoxicological and chemical evaluation of phenolic compounds in industrial effluents. Chemosphere 44, 1737–1747.

Guinea, E., Centellas, F., Brillas, E., Cañizares, P., Sáez, C., Rodrigo, M.A., 2009. Electrocatalytic properties of diamond in the oxidation of a persistent pollutant. Appl. Catal. B Environ. 89, 645–650.

Han, W., Zhong, C., Liang, L., Sun, Y., Guan, Y., Wang, L., Sun, X., Li, J., 2014. Electrochemical degradation of triazole fungicides in aqueous solution using TiO_2-NTs/SnO_2-Sb/PbO_2 anode: experimental and DFT studies. Electrochim. Acta 130, 179–186.

Homem, V., Santos, L., 2011. Degradation and removal methods of antibiotics from aqueous matrices – a review. J. Environ. Manage 92, 2304–2347.

Hurwitz, G., Pornwongthong, P., Mahendra, S., Hoek, E.M.V., 2014. Degradation of phenol by synergistic chlorine-enhanced photo-assisted electrochemical oxidation. Chem. Eng. J. 240, 235–243.

Kapalka, A., Fóti, G., Comninellis, C., 2009. The importance of electrode material in environmental electrochemistry: formation and reactivity of free hydroxyl radicals on boron-doped diamond electrodes. Electrochim. Acta 54, 2018–2023.

Karci, A., 2014. Degradation of chlorophenols and alkylphenol ethoxylates, two representative textile chemicals, in water by advanced oxidation processes: the state of the art on transformation products and toxicity. Chemosphere 99, 1–18.

Klauson, D., Babkina, J., Stepanova, K., Krichevskaya, M., Preis, S., 2010. Aqueous photocatalytic oxidation of amoxicillin. Catal. Today 151, 39–45.

Kong, X., Jiang, J., Ma, J., Yang, Y., Liu, W., Liu, Y., 2016. Degradation of atrazine by UV/chlorine: efficiency, influencing factors, and products. Water Res. 90, 15–23.

Li, S.-W., Lin, A.Y.-C., 2015. Increased acute toxicity to fish caused by pharmaceuticals in hospital effluents in a pharmaceutical mixture and after solar irradiation. Chemosphere 139, 190–196.

Lin, Z., Yao, W., Wang, Y., Yu, G., Deng, S., Huang, J., Wang, B., 2016. Perchlorate formation during the electro-peroxone treatment of chloride-containing water: effects of operational parameters and control strategies. Water Res. 88, 691–702.

Lizhang, W., Shengxiang, Y., Bo, W., Peng, L., Zhe'nan, L., Yuemin, Z., 2016. The influence of anode materials on the kinetics toward electrochemical oxidation of phenol. Electrochim. Acta 206, 270–277.

Locatelli, M.A.F., Sodré, F.F., Jardim, W.F., 2011. Determination of antibiotics in brazilian surface waters using liquid chromatography–electrospray tandem mass spectrometry. Arch. Environ. Contam. Toxicol. 60, 385–393.

Luo, Y., Guo, W., Ngo, H.H., Nghiem, L.D., Hai, F.I., Zhang, J., Liang, S., Wang, X.C., 2014. A review on the occurrence of micropollutants in the aquatic environment and their fate and removal during wastewater treatment. Sci. Total Environ. 473–474, 619–641.

Martín de Vidales, M.J., Millán, M., Sáez, C., Pérez, J.F., Rodrigo, M.A., Cañizares, P., 2015. Conductive diamond electrochemical oxidation of caffeine-intensified biologically treated urban wastewater. Chemosphere 136, 281–288.

Michael, I., Rizzo, L., McArdell, C.S., Manaia, C.M., Merlin, C., Schwartz, T., Dagot, C., Fatta-Kassinos, D., 2013. Urban wastewater treatment plants as hotspots for the release of antibiotics in the environment: a review. Water Res. 47, 957–995.

Miwa, D.W., Malpass, G.R.P., Machado, S.A.S., Motheo, A.J., 2006. Electrochemical degradation of carbaryl on oxide electrodes. Water Res. 40, 3281–3289.

Murugananthan, M., Latha, S.S., Bhaskar Raju, G., Yoshihara, S., 2011. Role of electrolyte on anodic mineralization of atenolol at boron doped diamond and Pt electrodes. Sep. Purif. Technol. 79, 56–62.

Oller, I., Malato, S., Sánchez-Pérez, J.A., 2011. Combination of advanced oxidation processes and biological treatments for wastewater decontamination - a review. Sci. Total Environ. 409, 4141–4166.

Orias, F., Perrodin, Y., 2013. Characterisation of the ecotoxicity of hospital effluents: a review. Sci. Total Environ. 454–455, 250–276.

Oturan, N., Trajkovska, S., Oturan, M.A., Couderchet, M., Aaron, J.-J., 2008. Study of the toxicity of diuron and its metabolites formed in aqueous medium during application of the electrochemical advanced oxidation process "electro-Fenton". Chemosphere 73, 1550–1556.

Panizza, M., Cerisola, G., 2009. Direct and mediated anodic oxidation of organic pollutants. Chem. Rev. 109, 6541–6569.

Pereira, G.F., El-Ghenymy, A., Thiam, A., Carlesi, C., Eguiluz, K.I.B., Salazar-Banda, G.R., Brillas, E., 2016. Effective removal of Orange-G azo dye from water by electro-Fenton and photoelectro-Fenton processes using a boron-doped diamond anode. Sep. Purif. Technol. 160, 145–151.

Puckowski, A., Mioduszewska, K., Łukaszewicz, P., Borecka, M., Caban, M., Maszkowska, J., Stepnowski, P., 2016. Bioaccumulation and analytics of

pharmaceutical residues in the environment: a review. J. Pharm. Biomed. Anal. 127, 232–255.
Quiroz, M.A., Sánchez-Salas, J.L., Reyna, S., Bandala, E.R., Peralta-Hernández, J.M., Martínez-Huitle, C.A., 2014. Degradation of 1-hydroxy-2,4-dinitrobenzene from aqueous solutions by electrochemical oxidation: role of anodic material. J. Hazard. Mater. 268, 6–13.
Radjenovic, J., Sedlak, D.L., 2015. Challenges and opportunities for electrochemical processes as next-generation technologies for the treatment of contaminated water. Environ. Sci. Technol. 49, 11292–11302.
Rickman, K.A., Mezyk, S.P., 2010. Kinetics and mechanisms of sulfate radical oxidation of beta-lactam antibiotics in water. Chemosphere 81, 359–365.
Rivera-Utrilla, J., Sánchez-Polo, M., Ferro-García, M.Á., Prados-Joya, G., Ocampo-Pérez, R., 2013. Pharmaceuticals as emerging contaminants and their removal from water. A review. Chemosphere 93, 1268–1287.
Sales, A.M.S., de Araújo, C.K.C., de Melo, J.V., Peralta-Hernandez, J.M., da Silva, D.R., Martínez-Huitle, C.A., 2013. Decontamination of real textile industrial effluent by strong oxidant species electrogenerated on diamond electrode: viability and disadvantages of this electrochemical technology. Appl. Catal. B Environ. 130–131, 112–120.
Santos, L.H.M.L.M., Araújo, A.N., Fachini, A., Pena, A., Delerue-Matos, C., Montenegro, M.C.B.S.M., 2010. Ecotoxicological aspects related to the presence of pharmaceuticals in the aquatic environment. J. Hazard. Mater 175, 45–95.
Särkkä, H., Bhatnagar, A., Sillanpää, M., 2015. Recent developments of electro-oxidation in water treatment — a review. J. Electroanal. Chem. 754, 46–56.
Silambarasan, S., Vangnai, A.S., 2016. Biodegradation of 4-nitroaniline by plant-growth promoting Acinetobacter sp. AVLB2 and toxicological analysis of its biodegradation metabolites. J. Hazard. Mater. 302, 426–436.
Singh, K., Arora, S., 2011. Removal of synthetic textile dyes from wastewaters: a critical review on present treatment technologies. Crit. Rev. Environ. Sci. Technol. 41, 807–878.
Sirés, I., Brillas, E., Oturan, M.A., Rodrigo, M.A., Panizza, M., 2014. Electrochemical advanced oxidation processes: today and tomorrow. A review. Environ. Sci. Pollut. Res. 21, 8336–8367.
Song, W., Chen, W., Cooper, W.J., Greaves, J., Miller, G.E., 2008. Free-radical destruction of beta-lactam antibiotics in aqueous solution. J. Phys. Chem. A 112, 7411–7417.
Sopaj, F., Rodrigo, M.A., Oturan, N., Podvorica, F.I., Pinson, J., Oturan, M.A., 2015. Influence of the anode materials on the electrochemical oxidation efficiency. Application to oxidative degradation of the pharmaceutical amoxicillin. Chem. Eng. J. 262, 286–294.
Tissot, G.B., Anglada, A., Dimitriou-Christidis, P., Rossi, L., Arey, J.S., Comninellis, C., 2012. Kinetic experiments of electrochemical oxidation of iohexol on BDD electrodes for wastewater treatment. Electrochem. Commun. 23, 48–51.
Van Doorslaer, X., Dewulf, J., Van Langenhove, H., Demeestere, K., 2014. Fluoroquinolone antibiotics: an emerging class of environmental micropollutants. Sci. Total Environ. 500–501, 250–269.
Vasconcelos, V.M., Ponce-de-León, C., Nava, J.L., Lanza, M.R.V., 2016. Electrochemical degradation of RB-5 dye by anodic oxidation, electro-Fenton and by combining anodic oxidation–electro-Fenton in a filter-press flow cell. J. Electroanal. Chem. 765, 179–187.
Zhang, J., Chang, V.W.C., Giannis, A., Wang, J.-Y., 2013. Removal of cytostatic drugs from aquatic environment: a review. Sci. Total Environ. 445–446, 281–298.